Journal of ELECTRONIC MATERIALS, Vol. 45, No. 11, 2016
DOI: 10.1007/s11664-016-4797-6

Effect of Copper Sulfide Nanoparticles on the Optical and Electrical Behavior of Poly(vinyl alcohol) Films

OMED GH. ABDULLAH[1,2,4] and SALWAN A. SALEEM[3]

1.—Department of Physics, Faculty of Science and Science Education, School of Science, University of Sulaimani, Sulaymaniyah, Kurdistan Region, Iraq. 2.—Development Centre for Research and Training (DCRT), University of Human Development, Sulaymaniyah, Kurdistan Region, Iraq. 3.—Department of Physics, College of Science, University of Mosul, Mosul, Iraq. 4.—e-mail: omed.abdullah@univsul.edu.iq

Polymer nanocomposite films based on poly(vinyl alcohol) (PVA) containing copper sulfide nanoparticles (CuS) were prepared using *in situ* chemical reduction and casting techniques. The synthesized nanocomposites were analyzed using x-ray diffraction (XRD), Fourier transform infrared spectroscopy (FTIR), scanning electron microscope, and ultraviolet–visible spectroscopy. The XRD pattern reveals that the CuS nanoparticles incorporated in the PVA showed a crystalline nature. The observed FTIR band shifts indicate the intermolecular interaction between the CuS nanoparticles and the PVA matrix. The absorbance of nanocomposite samples increased with increasing CuS concentration. The optical band gap energy was estimated using Tauc's formula and it decreased with increasing dopant concentration. The conductivity and dielectric behavior of the samples were studied over the frequency range of 300 Hz to 1 MHz in the temperature range of 30–110°C. The ac conductivity was found to increase with the increase of dopant concentration as well as frequency. Moreover, the variation of frequency exponent (s) indicated that the conduction mechanism was the correlated barrier hopping model. The experimental results reveal that the optical and electrical performance of PVA can be enhanced dramatically by the addition of a small amount of CuS nanoparticles. This improved properties of the PVA/CuS nanocomposite suggest uses in optoelectronic devices.

Key words: Polymer nanocomposites, PVA, copper sulfide, optical band gap, ac conductivity, dielectric constant

INTRODUCTION

The field of polymer nanocomposites has attracted strong interest in today's materials research in view of their wide applications in electronic and optical devices.[1] The optical absorption spectra of polymer nanocomposites provide essential information about the band structure and energy gap in polymer matrices.[2] It has been shown that the electrical, optical and structural properties of polymers can be suitably modified by the incorporation of a few weight percentages of inorganic filler in the polymer matrices.[3,4] The properties of particulate polymer nanocomposites mainly depend on the particle shape, size, and concentration, and the way in which the particles are dispersed and interact with the polymer matrix, which can achieve impressive enhancements of the polymer properties as compared with the pure polymers.[5]

The incorporation of functional nanoparticles in the polymer medium has been a subject of immense interest in recent years because of their uniquely promising properties and applications.[6]

Water-soluble poly(vinyl alcohol) (PVA) is one of the most promising polymers due to its unique properties such as high transmittance, easy processability, noncorrosive nature, and good thermal stability over a wide

(Received March 10, 2016; accepted July 7, 2016; published online July 28, 2016)

range of temperature,[7] making it an ideal matrix for optoelectronic applications.

Copper sulfide (CuS) has been reported as one of the most important *p*-type semiconductors in solar cells, and has been studied extensively, not only because of its excellent optical, electrical, and chemical properties at room temperature but also owing to its potential applications in many fields, such as corrosion science, solar energy converter, photocatalysis, and biosensors.[8–12] Therefore, significant efforts are being focused on the ability to prepare and control the nanoscale structures via innovative synthetic approaches.[13,14] A number of methods have been developed for the synthesis of CuS nanostructures including the solid-state reaction route,[15,16] sonochemical synthesis,[17,18] the microemulsions route,[19] the pickering emulsion route,[20] microwave irradiation techniques,[21,22] the hydrothermal route,[23,24] pyrolysis of single source precursors[25] and so on.

In this paper, we prepared CuS nanoparticles that were well dispersed in PVA polymer matrices film via *in situ* chemical reduction and casting techniques. The investigation focuses on the effect of synthesized CuS nanoparticles on the optical and electrical behavior of PVA polymer. The optical absorption spectroscopy is an established tool to investigate the effect of CuS on the band structure and electronic properties of PVA.[4] In addition, the study of dielectric properties as a function of temperature and frequency is a convenient method of investigating the structure of polymer nanocomposites.[26]

MATERIALS AND EXPERIMENTS

Materials

The chemicals used in this study were poly(vinyl alcohol) (PVA) $[C_2H_4O]_n$ (98%–99% hydrolyzed, low molecular weight), supplied by Alfa Aesar, as a capping, and distilled water was used as a solvent for the polymer. The salts used to prepare CuS nanoparticles were copper nitrate ($Cu(NO_3)_2$) with a molecular weight (241.54 g mol^{-1}) which was purchased from Merck, and sodium sulfide nonahydrate ($Na_2S{\cdot}9H_2O$) with a molecular weight (240.18 g mol^{-1}) purchased from Sigma-Aldrich. These materials were used without any purification.

Preparation of PVA/CuS Nanocomposite Films

Poly(vinyl alcohol) solution was prepared by dissolving 2 g of PVA in 30 mL distilled water with magnetic stirring for 1 h at 90°C until a clear homogenous viscous polymer solution was formed. Copper nitrate ($Cu(NO_3)_2$) as a source of cations and sodium sulfide (Na_2S) as a source of anions were separately dissolved in 5 mL distilled water with different molar concentrations (0.01 M, 0.02 M, 0.03 M, and 0.04 M) at room temperature. Different concentrations of nanosize CuS was prepared in PVA by adding the two solutions dropwise with a ratio of 1:1 to the homogeneous aqueous solution of PVA under stirring. The dissolved Cu^{2+} ions react with the released S^{2-} to form CuS nuclei. The PVA polymer acts as a stabilizer and a capping agent, which effectively protects the nanoparticles from aggregation.[27] The final solution turned deep blue, consistent with the color of the CuS covellite; thus, CuS nanoparticles were formed. To achieve maximum dispersion, the solutions were sonicated for 5 min. The homogeneous solutions were poured into Petri dishes 5 cm in diameter. The whole assembly was placed in a dust-free chamber maintained at 30°C, and the solvent was allowed to evaporate completely in air for 2 weeks to allow films to form. Then, the films were transferred into desiccators with silica gel for further drying. The prepared films were uniform with a thickness in the range of 40–60 μm.

Characterization Techniques

The x-ray diffraction (XRD) patterns of the prepared pure PVA and PVA/CuS polymer nanocomposite films were collected using an x-ray diffractometer (X'PERT-PRO) equipped with CuKα radiation (λ = 0.154 nm) in the 2θ range 10°–60° at a scanning rate of 2° min^{-1}. The Fourier transform infrared (FTIR) spectra of the pure and doped PVA films were analyzed in the range 400–4000 cm^{-1} using a Perkin Elmer instrument in transmission mode with a resolution of 1.0 cm^{-1}. Scanning electron microscope (SEM) micrographs were taken using a CamScan 3200 to investigate the morphological appearance of the prepared nanocomposite samples. Optical absorption studies were carried out in the wavelength range 190–1100 nm using a double beam ultraviolet–visible (UV–Vis) spectrophotometer (Perkin Elmer, Lambda 25). The obtained data were further analyzed to estimate the optical band gap energy of the prepared films.

The electrical properties were measured using a precision inductance–capacitance–resistance (LCR) meter (Agilent/HP 4284A) operating at a frequency range from 300 Hz to 1 MHz and in the temperature range 30–110°C. The 2.5-cm-diameter films were sandwiched between two aluminum electrodes under spring pressure. In order to measure the temperature-dependent conductivity, strip heaters were used to heat a chamber and a K-type thermocouple (accuracy ±0.1°C) was used to measure the temperature of the sample.

RESULTS AND DISCUSSION

X-ray Diffraction (XRD) Analysis

The structural identification of the PVA/CuS nanocomposite was carried out using XRD analysis. Figure 1 shows the XRD patterns of pure and doped PVA films with 0.04 M CuS. The broad peak observed at $2\theta \approx 19.26°$ for both samples is due to the PVA matrix.[28,29] The observed additional diffraction peaks of the nanocomposite film at scattering angles 2θ = 29.61°, 32.08°, 33.32°, and 48.31° correspond to

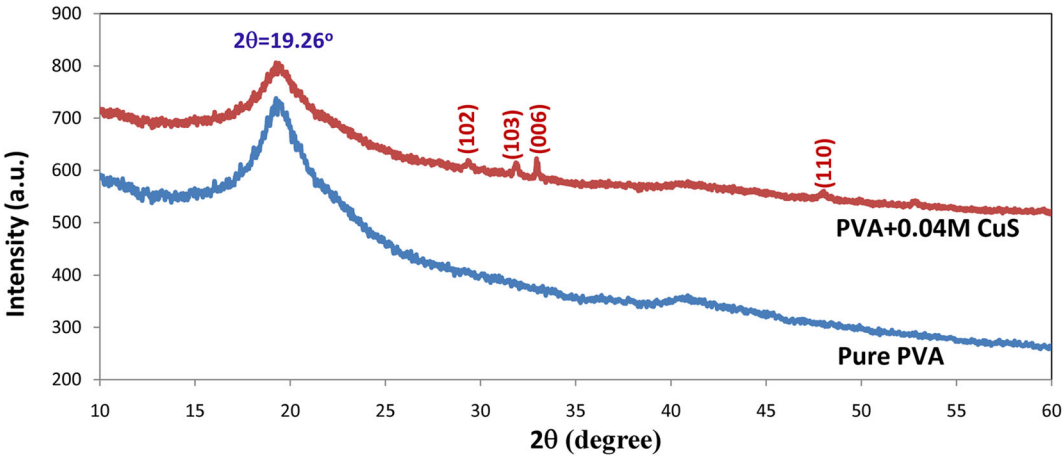

Fig. 1. The x-ray diffraction patterns of pure PVA, and a PVA +0.04 M CuS nanocomposite.

(102), (103), (006), and (110) crystal planes, respectively.[30,31] The position and the relative intensities of these peaks are well matched with the standard data recorded in the JCPDS card no. 06-0464: $a = b = 3.793$ Å, $c = 16.347$ Å, space group $P6_3/mmc$, with hexagonal unit cells (covellite).[32–34] The average grain size D of CuS in nanocomposite films was calculated using the well-known Debye–Scherrer equation.[35]

$$D = \frac{0.9\lambda}{\beta \cos\theta} \quad (1)$$

where λ is the x-ray wavelength (in nm), β is the peak width of the diffraction peak at half-maximum height (in radians), and θ is the diffraction angle of the peak.

The obtained particle size of the CuS nanoparticles embedded in PVA polymer films was in the range 39.50–46.54 nm. The results indicated that the average particle sizes gradually increased with increasing CuS concentration, which may be attributed to the nanoparticles aggregation in the samples with increasing CuS amount.

FTIR Spectroscopy Analysis

FTIR analysis was performed to determine the possible intermolecular interaction between the PVA matrix and CuS nanoparticles, which can be deduced from the band shifting.[4] The FTIR spectra for pure PVA and PVA/0.04 M CuS nanocomposite films are shown in Fig. 2. Both spectra exhibit the characteristic absorption bands of pure PVA. A strong broad absorption band observed between 3171 cm^{-1} and 3460 cm^{-1} is assigned to a hydroxyl group and the bonded O–H stretching vibration of PVA.[36] The bands observed at 2942 cm^{-1} and 1092 cm^{-1} suggest the presence of C-H stretching and C-O stretching vibrations on the PVA backbone.[37] The two peaks at 1427 cm^{-1} and 1331 cm^{-1} are due to the stretching vibrations of CH_3 and CH_2, respectively.[38]

There is no appearance of an additional peak in the PVA/CuS nanocomposite spectra; however, a slight shift to a lower wavenumber in the peak position of the band corresponds to the O–H stretch and C–O–C stretch vibrations of PVA, indicating a physical interaction between the CuS nanoparticles and the hydroxyl groups of PVA.

Scanning Electron Microscopy (SEM) Analysis

The morphology of PVA/CuS polymer nanocomposites was characterized using SEM imaging at the fracture surface of the nanocomposite films. Figure 3 shows the surface morphology of different compositions of PVA/CuS polymer nanocomposite films. The SEM images show CuS nanoparticles (white spots) homogeneously dispersed within the polymer matrix. It is also clear that the increase in copper nitrate and sodium sulfide concentrations causes the development of CuS average particle sizes due to the agglomeration of the nanoparticles.

Optical Characterization

The study of the optical absorption edge in the UV and visible regions provides very useful information to elucidate the optical transitions and electronic band structure of the materials.[2,39] The law of the absorption of light was used to calculate the absorption coefficient (α) according to Lambert's law, which can be calculated from the optical absorbance spectrum using the relationship:

$$\alpha(\lambda) = 2.303\frac{A(\lambda)}{d} \quad (2)$$

where d is the sample thickness, λ is the wavelength of the incident photons and A is the absorbance defined by $A = \log(I_o/I)$, where I_o and I are the intensities of the incident and transmitted beams, respectively.

The UV/Vis spectrophotometric scans for all the samples were measured in the wavelength range

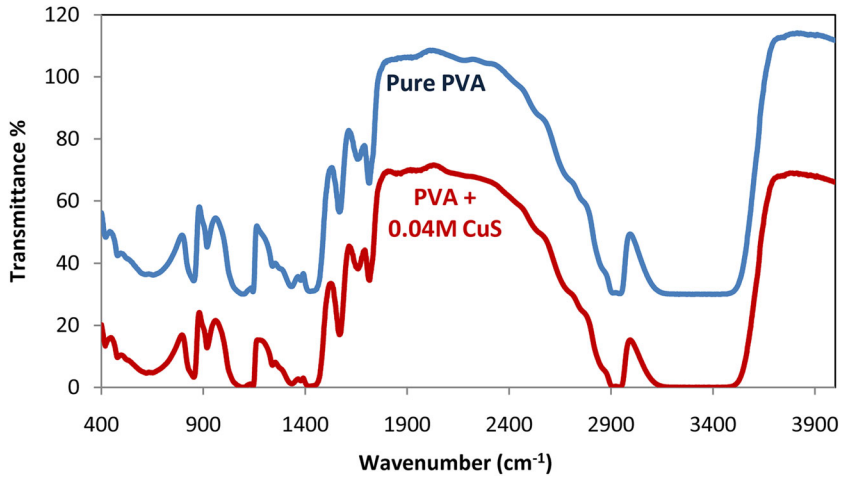

Fig. 2. FTIR spectra of pure PVA, and PVA/0.04 M CuS nanocomposite films.

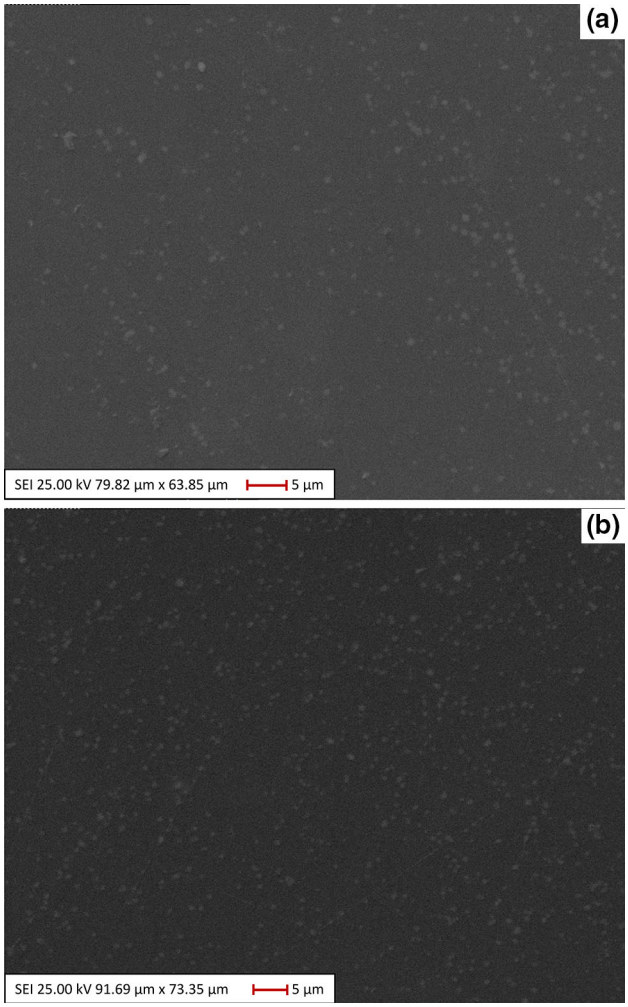

Fig. 3. SEM images of PVA/CuS nanocomposite film (a) 0.02 M CuS, (b) 0.04 M CuS.

190–1100 nm. The variations of absorbance with wavelength for all the prepared films are shown in Fig. 4. The nanocomposites sample shows a notable absorption in the near infrared region (characteristic of covellite) due to the localized surface plasma resonances of the CuS nanoparticles.[40,41] Meanwhile, the absorbance gradually enhanced with the increase of the CuS content, indicating the good dispersion of CuS in the polymer matrices.[36,42] Overall, the PVA/CuS nanocomposite shows high absorbance compared to the pure PVA polymer.

Further, the observed shifts of the spectra towards the higher wavelength side with the increasing concentration of CuS indicates a change in the optical band gap of the films. This shift in the absorbance spectra towards the higher wavelength side suggests a reduction in the band gap value.[43]

The energy band gap of the films was estimated using fundamental absorption, which refers to the electron excitation between the valence band and conduction band.[43] The energy band gap E_g of the films was calculated using the Tauc/David–Mott model[44,45] described by:

$$\alpha h\upsilon = \beta\left(h\upsilon - E_g\right)^{\gamma} \tag{3}$$

where $h\upsilon$ is the incident photons energy, β is a proportional constant related to the extent of the band tailing and depends on the transition probability, and γ is the power which characterizes the nature of electron transition process in the K-space. Specifically, γ is 1/2, 3/2, 2 and 3 for transitions direct allowed, direct forbidden, indirect allowed and indirect forbidden, respectively.[46,47]

Figure 5 shows the plots of $(\alpha h\upsilon)^2$ versus photon energy $h\upsilon$ for all the prepared films. The E_g values were determined by extrapolating the linear portion of the curves to zero absorption.[35] The band gap E_g of the pure PVA was calculated to be 6.27 eV, and was found to decrease by increasing the CuS content to 5.375 eV, 5.25 eV, 5.00 eV, and 4.776 eV for 0.01 M, 0.02 M, 0.03 M, and 0.04 M of CuS, respectively. Many other researchers have also

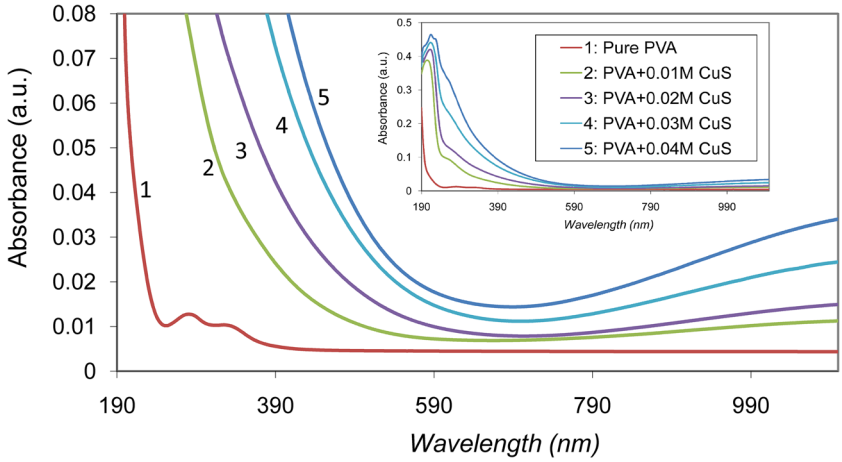

Fig. 4. Absorbance spectra of the pure PVA, and PVA/CuS nanocomposite films.

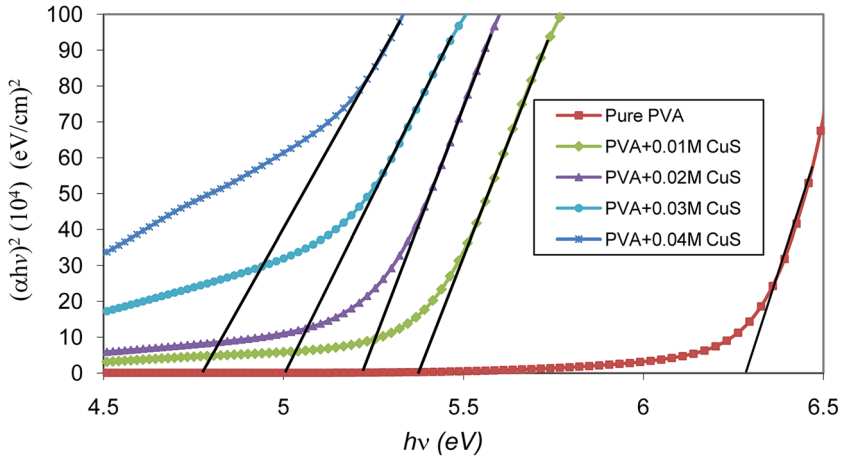

Fig. 5. The plots of $(\alpha h\nu)^2$ versus $(h\nu)$ for PVA/CuS nanocomposite films.

reported the decrease of the optical band gap of PVA with increasing the weight percent of the nanoparticles in the systems PVA/ZnS,[47] PVA/Cr_2O_3,[48] PVA/CaF_2,[49] and PVA/Ag.[50]

The gradual decrease in the value of E_g by increasing the CuS concentration may be attributed to the generation of localized states (increase in the number of traps) between the highest occupied molecular orbital and lowest unoccupied molecular orbital energy bands, making the lower energy transitions feasible.[51,52] The reduction in energy gap value in PVA after embedding CuS makes them efficient materials for optoelectronic devices, since such those requiring band gap tunability.[46]

Electrical Characterization

The values of ac conductivity (σ_{ac}) of the present polymer nanocomposites have been calculated to obtain a better understanding of the conduction process. The frequency dependence of σ_{ac} at room temperature is plotted in Fig. 6 for the prepared samples. The ac conductivity was calculated using the following relationship[53]:

$$\sigma_{ac} = \frac{dG_s}{A} \tag{4}$$

where G_s is the measured conductance and A is the electrode cross-sectional area. As shown in Fig. 6, the conductivity appears to be frequency-dependent. In the low-frequency range, conductivity tends to acquire constant values approaching its dc value, while a critical value varies exponentially with frequency.[54] This type of behavior is common in disordered solids, appears to be in accordance with the so-called 'ac universality law', and is considered as a strong indication of charge migration via the hopping mechanism.[26,55] The increase of σ_{ac} with increasing temperature suggested the thermally activated process from different localized states in the band gap.[56] Meanwhile, the increase of ac conductivity with increasing CuS concentration can be attributed to the increasing of charge migration in the matrix.[38]

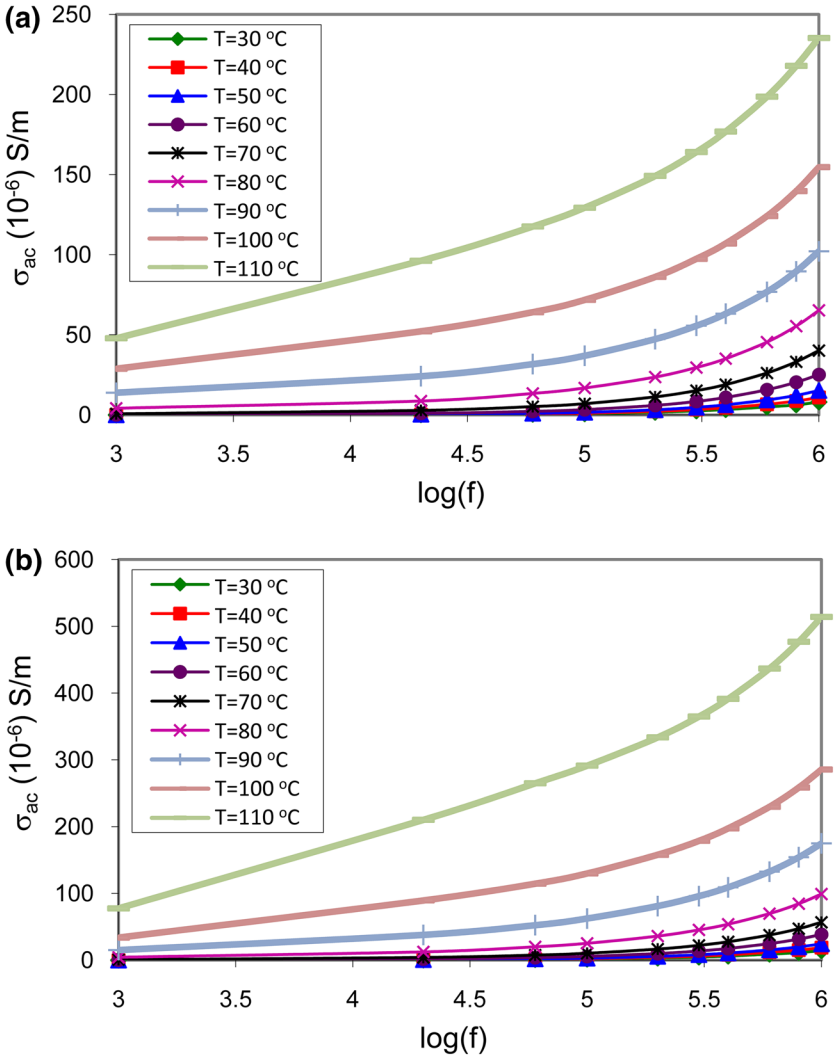

Fig. 6. The ac-conductivity as a function of frequency at different temperatures for (a) pure PVA and (b) PVA/0.04 M CuS nanocomposites.

It is well known that, in highly disordered systems, over a wide range of frequencies, the ac-conductivity σ_{ac} obeys Jonscher's universal power law[57]:

$$\sigma_{ac} = B\omega^s \tag{5}$$

where B is a frequency-independent, temperature-dependent parameter, $\omega = 2\pi f$ is the angular frequency, and s is the dimensionless frequency exponent, which is a measure of the degree of interaction with the values 0 and 1 for an ideal Debye dielectric dipolar-type and an ideal ionic-type crystal, respectively. The typical values of s, between 0 and 1 indicate the charge–carrier interactions during the hopping conduction mechanism.[58,59]

The frequency-dependent ac-conductivity (σ_{ac}) data have been fitted by using Jonscher's universal power law, as shown in Fig. 7. The value of s can be obtained from the slopes of log (σ_{ac}) versus log (ω) for all samples at different temperatures. The obtained values of s versus temperature are presented in Fig. 8. The value of the frequency exponent s can characterize the type of electrical conduction mechanism. Many theoretical models have been put forward to explain the behavior of the s value.[38]

It is clear from Fig. 8 that the value of s has a higher value at room temperature and decreases with increasing temperature to a minimum value. According to the correlated barrier hopping (CBH) model, the value of s ranges from 0.7 to 1 at room temperature, and should show a decreasing trend with increasing temperature.[56] This description is in a good agreement with the obtained experimental results; therefore, based on the CBH model, ac-conductivity σ_{ac} can be explained in terms of the hopping of electrons between pairs of localized states at the Fermi level.[38]

The variation of dielectric constant (ε'), and dielectric loss factor (ε'') with frequency have proven to be a very useful tool to study the structure, dynamics and relaxations of polymeric systems. The

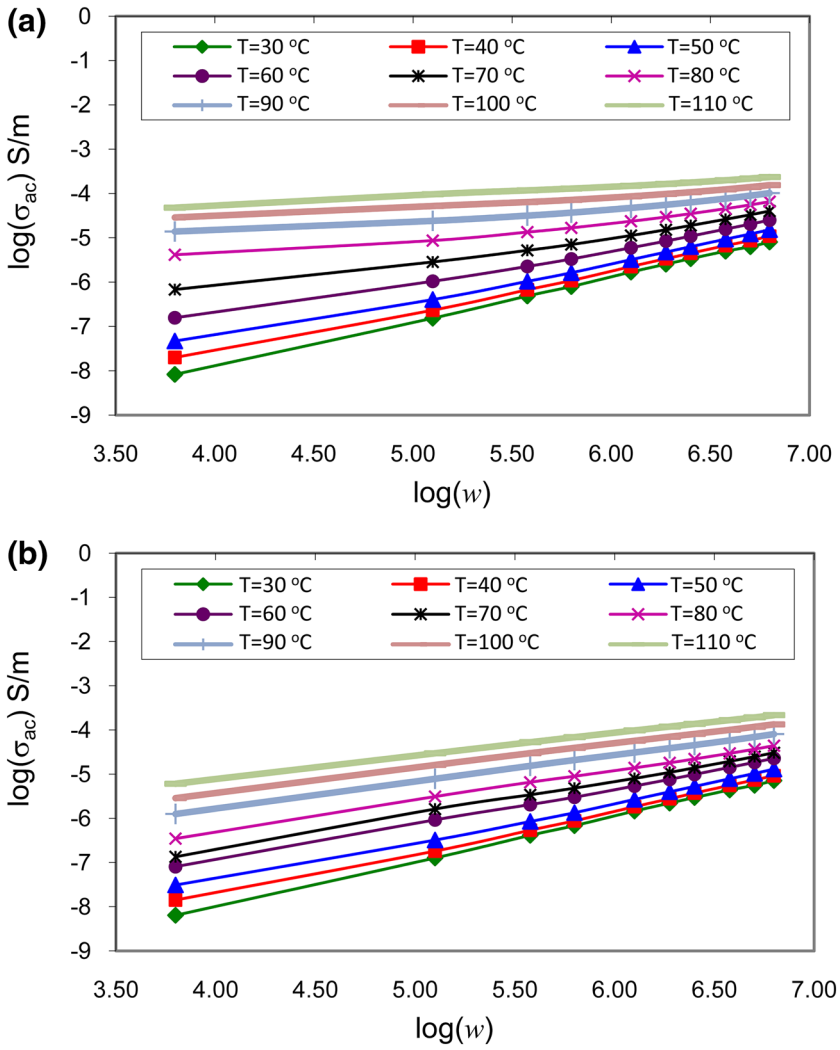

Fig. 7. Variation of log (σ_{ac}) with log (w) for (a) pure PVA, (b) PVA/CuS 0.04 M.

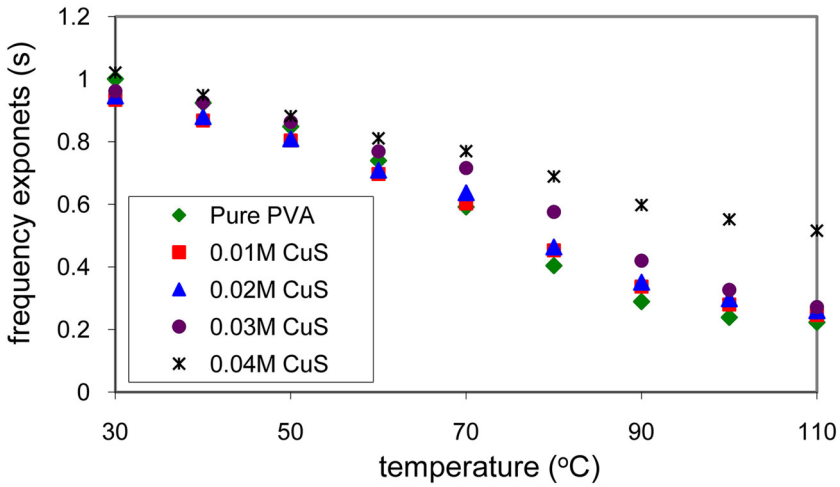

Fig. 8. The frequency exponents versus temperature for PVA/CuS polymer nanocomposites films.

dielectric constant (ε') and dielectric loss (ε'') were evaluated using the two equations:

$$\varepsilon' = \frac{C}{C_o} = \frac{Cd}{\varepsilon_o A} \tag{6}$$

$$\varepsilon'' = \frac{\sigma_{ac}}{\varepsilon_o \omega} \tag{7}$$

where C_o is the vacuum capacitance of any configuration of electrodes and C is the capacitance with dielectric material filling the space, and $\varepsilon_o = 8.85 \times 10^{-12}$ F/m is the permittivity of free space. The dielectric constants have been analyzed in terms of temperature, frequency, and CuS content. Figure 9a and b depicts the variation of dielectric constant (ε') with respect to frequency for pure PVA and PVA/CuS nanocomposite at 0.04 M CuS content, respectively, at different temperatures. The measurements were made isothermally in the temperature range 30–110°C in the frequency range from 300 Hz to 1 MHz.

The results indicate that, at low frequencies, the dielectric constant attained higher values in all samples, which reduced rapidly with frequency. It is clear that (ε') decreases monotonically with increasing frequency and attains a constant value at higher frequencies. Similar behaviour has been observed for different polar polymer composites.[60] This is because, for polar polymers, the initial value of the dielectric constant (ε') is high, but as the frequency increases the value begins to drop, which could be due to the dipoles not being able to follow the field variation at higher frequencies.[38] Hence,the dielectric constant (ε') decreases with the increase of the frequency in all the PVA samples.[61,62] Also, it has been found that the value of the dielectric constant (ε') increases gradually due to the increase of CuS in the PVA polymer matrix. Enhanced values of (ε') can be attributed to increases in dipolar polarization, especially in the high-frequency region.[63,64]

The increase in (ε') with temperature can be ascribed to the fact that the orientational

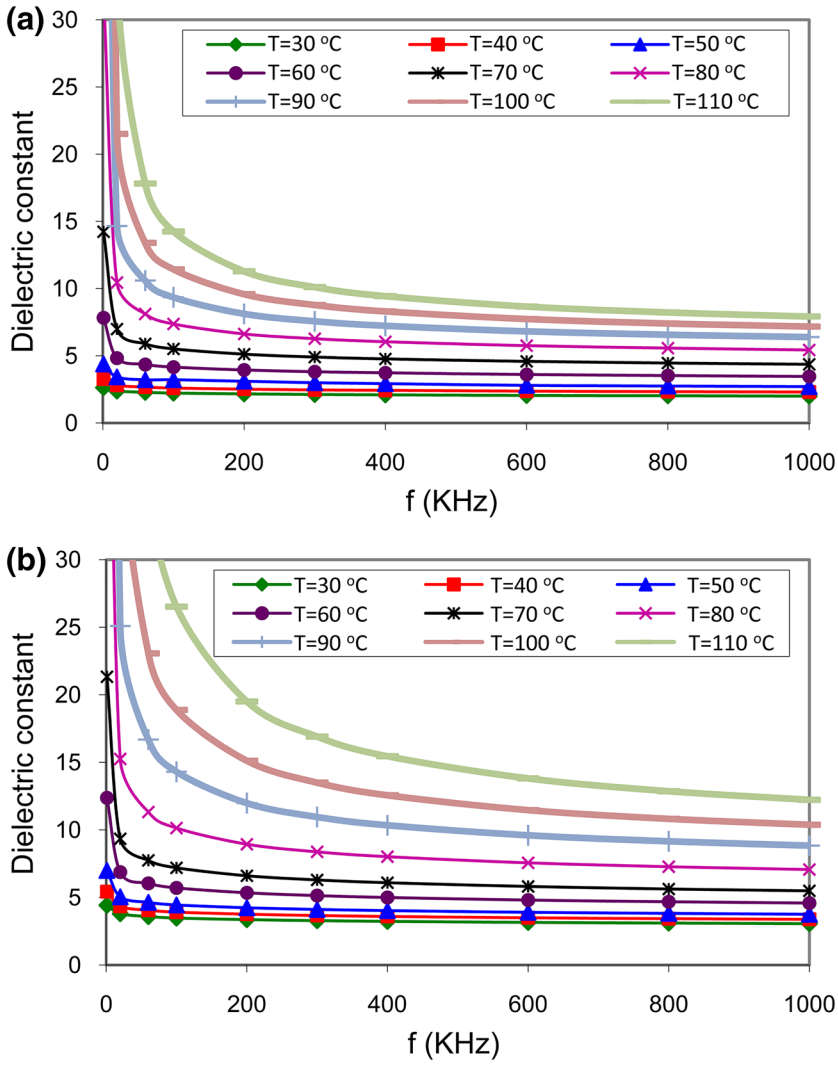

Fig. 9. The dielectric constant (ε') against frequency at different temperature for (a) pure PVA, (b) PVA/CuS 0.04 M.

polarization is related to the thermal motion (vibration) of the molecules, so dipoles cannot orient themselves at lower temperatures. When the temperature increases, the orientation of dipoles is facilitated, which leads to increases in the value of orientational polarization and, consequently, the value of the dielectric constant ε'.[65]

The dielectric loss factor ε'' versus frequency for various samples are shown in Fig. 10. The nature of the variation of dielectric loss ε'' with frequency is the same as that of the dielectric constant ε' with frequency. It is clear that ε'' decreases exponentially with the increase in frequency and attains a constant value at higher frequencies due to the polar nature of the PVA polymer. At low frequencies, the dipoles have sufficient time to orient themselves in the electric field before changing their direction and, consequently, the dielectric loss is very high.[59] However, at higher frequency, the polymer dipoles cannot follow the field variation, leading to a decrease in the dielectric loss value. This result indicates the lossless nature of the samples at higher frequencies. Moreover, these results suggest that the dc-conductivity process is more significant than the interfacial polarization in the present samples.[66] The higher value of ε'' at the low-frequency range could be due to the the existence of mobile charges within the polymer backbone, while the increases in ε'' value with CuS content can be understood in terms of electrical conductivity which is associated with the dielectric loss.[67]

The dispersion behavior of the dielectric constant and dielectric loss for the investigated samples are significant for practical purposes because the dispersion factor plays an important role in designing optical devices, particularly in the field of optical communication.[68] It is also evident that the values of both ε' and ε'' increased steeply with increasing temperature and CuS content. Increases of dielectic constants and dielectric loss with increases in

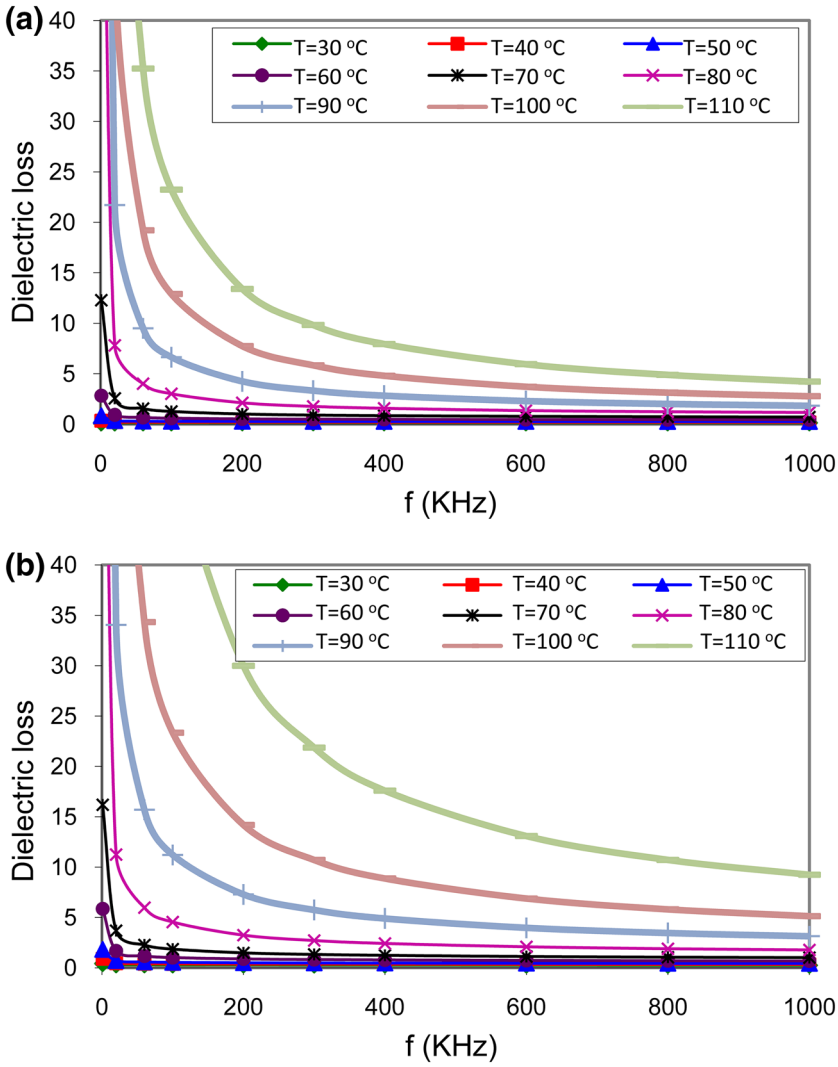

Fig. 10. Variation of dielectric loss (ε'') against frequency at different temperatures for (a) pure PVA, (b) PVA/CuS 0.04 M.

nanoparticle content have also been reported for CuS nanoparticles incorporated in polypyrrole matrices.[69]

CONCLUSIONS

Polymer nanocomposites have been prepared from CuS-embedded poly(vinyl alcohol) (PVA) using the solution casting technique. XRD analysis confirmed the formation of CuS nanocrystals embedded in the PVA film with an average particle size between 39.50 nm and 46.54 nm. FTIR analysis showed that the interaction between the CuS nanoparticles and the PVA chains occurred at the hydroxyl (O–H) and ether (C–O–C) groups. The characteristic properties of the prepared samples have been studied using UV–Vis spectroscopy and dielectric spectroscopy. The reduction in the optical energy gap value of the PVA after embedding CuS make it an efficient material for optoelectronic devices. Also, the temperature dependence of the frequency exponent in the Jonscher formula suggests that the conduction mechanism can be explained according to the CBH model. Moreover, the increases in ac conductivity, dielectric constant, and dielectric loss of the nanocomposite samples corroborate the enhanced electrical behavior of PVA with increasing the embedded CuS nanoparticles.

ACKNOWLEDGEMENTS

The authors desire to thank the University of Sulaimani, for providing financial support for this research. The authors gratefully acknowledge the Ministry of Science and Technology for the facility in their laboratories.

REFERENCES

1. M. Bulinski, V. Kuncser, C. Plapcianu, S. Krautwald, H. Franke, P. Rotaru, and G. Filoti, *J. Phys. D Appl. Phys.* 37, 2437 (2004).
2. OGh Abdullah and S.A. Hussen, *Adv. Mater. Res.* 383, 3257 (2012).
3. S.Y. Fu, X.Q. Feng, B. Lauke, and Y.W. Mai, *Compos. B* 39, 933 (2008).
4. S.F. Bdewi, OGh Abdullah, B.K. Aziz, and A.A.R. Mutar, *J. Inorg. Organomet. Polym. Mater.* 26, 326 (2016).
5. S.R. Chauhan and S. Thakur, *Mater. Des.* 51, 398 (2013).
6. J. Xu, X. Cui, J. Zhang, H. Liang, H. Wang, and J. Li, *Bull. Mater. Sci.* 31, 189 (2008).
7. I. Saini, J. Rozra, N. Chandak, S. Aggarwal, P.K. Sharma, and A. Sharma, *Mater. Chem. Phys.* 139, 802 (2013).
8. J. Guan, J. Peng, and X. Jin, *Anal. Methods* 7, 5454 (2015).
9. Y. Hong, J. Zhang, F. Huang, J. Zhang, X. Wang, Z. Wu, Z. Lin, and J. Yu, *J. Mater. Chem. A* 3, 13913 (2015).
10. Y. Kim and D. Walsh, *Nanoscale* 2, 240 (2010).
11. S. Yu, J. Liu, W. Zhu, Z.T. Hu, T.-T. Lim, and X. Yan, *Sci. Rep.* 5, 16369 (2015).
12. L. Zhang, Y. Li, Z. Jin, J.C. Yu, and K.M. Chan, *Nanoscale* 7, 12614 (2015).
13. K. Ariga, Y. Yamauchi, G. Rydzek, Q. Ji, Y. Yonamine, K.C.W. Wu, and J.P. Hill, *Chem. Lett.* 43, 36 (2014).
14. K. Ariga, Q. Ji, W. Nakanishi, and J.P. Hill, *J. Inorg. Organomet. Polym.* 25, 466 (2015).
15. Y. Ni, F. Wang, H. Liu, Q. Zuo, Z. Xu, J. Hong, and X. Ma, *Chin. J. Inorg. Chem.* 19, 1197 (2003).
16. H. Wang, X. Lu, Y. Zhao, and C. Wang, *Mater. Lett.* 60, 2480 (2006).
17. H. Wang, J.R. Zhang, X.N. Zhao, S. Xu, and J.J. Zhu, *Mater. Lett.* 55, 253 (2002).
18. H. Xu, W. Wang, and W. Zhu, *Mater. Lett.* 60, 2203 (2006).
19. X. Dong, D. Potter, and C. Erkey, *Ind. Eng. Chem. Res.* 41, 4489 (2002).
20. Y. He and K. Li, *J. Colloid Interface Sci.* 306, 296 (2007).
21. Y. Ni, H. Liu, F. Wang, G. Yin, J. Hong, X. Ma, and Z. Xu, *Appl. Phys. A* 79, 2007 (2004).
22. X.H. Liao, N.Y. Chen, S. Xu, S.B. Yang, and J.J. Zhu, *J. Cryst. Growth* 252, 593 (2003).
23. H. Ji, J. Cao, J. Feng, X. Chang, X. Ma, J. Liu, and M. Zheng, *Mater. Lett.* 59, 3169 (2005).
24. P. Roy and S.K. Srivastava, *Mater. Lett.* 61, 1693 (2007).
25. T.H. Larsen, M. Sigman, A. Ghezelbash, R.C. Doty, and B.A. Korgel, *J. Am. Chem. Soc.* 125, 5638 (2003).
26. H.N. Chandrakala, B. Ramaraj, Shivakumaraiah, G.M. Madhu, and Siddaramaiah, *J. Alloys Compd.* 551, 531 (2013).
27. P.K. Khanna, R. Gokhale, V.V.V.S. Subbarao, A.K. Vishwanath, B.K. Das, and C.V.V. Satyanarayana, *Mater. Chem. Phys.* 92, 229 (2015).
28. S. Sarma and P. Datta, *Nanosci. Nanotechnol. Lett.* 2, 261 (2010).
29. R.P. Chahal, S. Mahendia, A.K. Tomar, and S. Kumar, *J. Alloys Compd.* 538, 212 (2012).
30. K. Tezuka, W.C. Sheets, R. Kurihara, Y.J. Shan, H. Imoto, T.J. Marks, and K.R. Poeppelmeier, *Solid State Sci.* 9, 95 (2007).
31. C. Deng, X. Ge, H. Hu, L. Yao, C. Han, and D. Zhao, *Cryst. Eng. Comm.* 16, 2738 (2014).
32. Z. Li, L. Mi, W. Chen, H. Hou, C. Liu, H. Wang, Z. Zheng, and C. Shen, *Cryst. Eng. Comm.* 14, 3965 (2012).
33. M. Tanveer, C. Cao, Z. Ali, I. Aslam, F. Idrees, W.S. Khan, F.K. But, M. Tahira, and N. Mahmood, *Cryst. Eng. Comm.* 16, 5290 (2014).
34. R.V. Kumar, O. Palchik, Y. Koltypin, Y. Diamant, and A. Gedanken, *Ultrason. Sonochem.* 9, 65 (2009).
35. OGh Abdullah, D.A. Tahir, and K. Kadir, *J. Mater. Sci.: Mater. Electron.* 26, 6939 (2015).
36. OGh Abdullah, Y.A.K. Salman, and S.A. Saleem, *Phys. Mater. Chem.* 3, 18 (2015).
37. Z. Ali, H. Youssef, and T. Afify, *Polym. Compos.* 29, 1119 (2008).
38. OGh Abdullah, Y.A.K. Salman, and S.A. Saleem, *J. Mater. Sci.: Mater. Electron.* 27, 3591 (2016).
39. A.U. Ubale, K.S. Chipade, M.V. Bhute, P.P. Raut, G.P. Malpe, Y.S. Sakhare, and M.R. Belkhedkar, *Int. J. Mater. Chem.* 2, 165 (2012).
40. X. Liu, Q. Ren, F. Fu, R. Zou, Q. Wang, G. Xin, Z. Xiao, X. Huang, Q. Liu, and J. Hu, *Dalton Trans.* 44, 10343 (2015).
41. Y. Du, Z. Yin, J. Zhu, X. Huang, X.J. Wu, Z. Zeng, Q. Yan, and H. Zhang, *Nat. Commun.* 3, 1177 (2012).
42. A.A. Ziabari and F.E. Ghodsi, *Sol. Energy Mater. Sol. Cells* 105, 249 (2012).
43. M. Madani, *Curr. Appl. Phys.* 11, 70 (2011).
44. N.F. Mott and E.A. Davis, *Electronic Processes in Non-crystalline Materials*, 1st ed. (Oxford: Oxford University Press, 1979), p. 34.
45. X. Li, H. Zhu, J. Wei, K. Wang, E. Xu, Z. Li, and D. Wu, *Appl. Phys. A* 97, 341 (2009).
46. OGh Abdullah, S.B. Aziz, K.M. Omer, and Y.M. Salih, *J. Mater. Sci.: Mater. Electron.* 26, 5303 (2015).
47. U. Baishya and D. Sarkar, *Bull. Mater. Sci.* 34, 1285 (2011).
48. A. Hassen, A.M. El Sayed, W.M. Morsi, and S. El-Sayed, *J. Appl. Phys.* 112, 093525 (2012).
49. O. Nakhaei, N. Shahtahmassebi, M. Rezaeeroknabadi, and M.M.B. Mohagheghi, *Sci. Iran. F* 19, 1979 (2012).
50. M. Ghanipour and D. Dorranian, *J. Nanomater.* 2013, 1 (2013). doi:10.1155/2013/897043.
51. H.M. Zidan, *J. Appl. Polym. Sci.* 88, 104 (2003).
52. S.A. Sbeih and A.M. Zihlif, *J. Phys. D Appl. Phys.* 24, 145405 (2009).
53. J.C. Dyre and T.B. Schroder, *Rev. Mod. Phys.* 72, 873 (2000).

54. G.C. Psarras, *J. Polym. Sci. Part B: Polym. Phys.* 45, 2535 (2007).
55. G.C. Psarras, *Compos. Part A: Appl. Sci. Manuf.* 37, 1545 (2006).
56. K. Ulutas, D. Deger, and S. Yakut, *J. Phys. Conf. Ser.* 417, 012040 (2013).
57. J. Yang, X.J. Meng, M.R. Shen, L. Fang, J.L. Wang, T. Lin, J.L. Sun, and J.H. Chu, *J. Appl. Phys.* 104, 104113 (2008).
58. A.K. Jonscher, *J. Mater. Sci.* 13, 553 (1978).
59. S.B. Aziz and Z.H.Z. Abidin, *Mater. Chem. Phys.* 144, 280 (2014).
60. P.B. Bhargav, V.M. Mohan, A.K. Sharma, and V.V.R.N. Rao, *Curr. Appl. Phys.* 9, 165 (2009).
61. V. Raja, A.K. Sharma, and V.V.R.N. Rao, *Mater. Lett.* 58, 3242 (2004).
62. T. Blythe and D. Bloor, *Electrical Properties of Polymers*, 2nd ed. (Cambridge: Cambridge University Press, 2005), p. 48.
63. D. Nwabunma and T. Kyu, *Polyolefin Composites* (New York: Wiley, 2008).
64. M. Trihotri, U.K. Dwivedi, F.H. Khan, M.M. Malik, and M.S. Qureshi, *J. Non-Cryst. Solids* 421, 1 (2015).
65. P.K. Khare and S.K. Jain, *Bull. Mater. Sci.* 23, 17 (2000).
66. B.G. Soares, M.E. Leyva, G.M.O. Barra, and D. Khastgir, *Eur. Polym. J.* 42, 676 (2006).
67. S.A. Mohamed, A.A. Al-Ghamdi, G.D. Sharma, and M.K. El Mansy, *J. Adv. Res.* 5, 79 (2014).
68. S.B. Aziz, R.T. Abdulwahid, H.A. Rsaul, and H.M. Ahmed, *J. Mater. Sci.: Mater. Electron.* 27, 4163 (2016).
69. M.T. Ramesan, *J. Appl. Polym. Sci.* 128, 1540 (2013).